Preparation of Anti-bacterial Biocomposite Nanofibers Fabricated by Electrospinning Method

Ömer KESMEZ*

Department of Chemistry, Faculty of Science, Akdeniz University, 07058 Antalya, Turkey.

Abstract: Developing technology and increasing the number of living creatures on Earth increase the demand for biomaterials each passing day. Recently, biocomposites and biodegradable biomaterials have begun to attract attention in many areas of use. Electrospinning technique is preferred as a quite consolidated technique in the production of outstanding polymer and/or nanofiber matrixes. However, obtained biocomposite nanofibers can cause microbiological infections during or after their usage. Therefore, it is very important that such materials have controlled antibacterial properties. In this study, Hydroxyapatite (HAp), known as biocompatible and bioactive, was firstly synthesized by wet precipitation method. Molecular structure of obtained HAp particles was researched by Fourier Transform Infrared Spectroscopy (FT-IR), its crystal structure was analyzed by X-ray Diffraction analysis (XRD) and its morphology was investigated by Scanning Electron Microscopy (SEM). HAp particles were combined with a mixture of biodegradable polylactic acid (or polylactide, PLA) and polycaprolactone (PCL) and biocomposite nanofibers were prepared by electrospinning method by loading chitosan and /or silver-based inorganic antimicrobial agent in different proportions to this composite structure. Molecular structure of PLA-PCL polymer matrix was investigated by FT-IR analysis. The obtained biocomposites are characterized morphology (SEM analysis), thermal behavior (TGA analysis) and mechanical properties. In vitro degradation test is performed to evaluate anti-bacterial biocomposite nano-fibers biodegradability. The anti-bacterial efficiency of biocomposite nano-fibers containing chitosan and/or Ag^+ in different proportions was investigated against *Escherichia coli* (Gram-negative) and *Staphylococcus aureus* (Gram-positive) bacteria. The results showed increasing mechanical properties and thermal stability. Biocomposite nano-fibers containing 1% chitosan and 0.25% Ag^+ were found to have ≥4.78 log reduction and ≥99.99% reduction in the bacterial population against the tested bacterial species and showed strong antibacterial properties. It was also observed that the combination of Ag^+ and chitosan may show synergistic effects. The results of the study confirm the great potential of biodegradable, biocompatible and bioactive fibers for antibacterial application.

*Corresponding author. E-mail: omerkesmez@akdeniz.edu.tr.
Tel: +90 (242) 310 2301. Fax: +90 (242) 310 2294.

INTRODUCTION

The increase in the number of people living on Earth and the increase in the proportion of the elderly population in the society in parallel with this increase stimulates the demand for biomaterials (1). Facial trauma, bone resection due to cancer, periodontal diseases, bone

atrophy after tooth extraction cause defects on bone and other tissues as a result of various accidents and these problems often do not heal spontaneously (2). Therefore, a variety of medical devices and/or biomaterials are needed for these conditions.

Many medical technologies include the usage of synthetic materials in many fields, from materials used in surgical procedures to scaffolds for tissue engineering. Some materials used in the medical field do not show the biodegradable property (3–5). The major disadvantage of these materials is that they require removal from the implanted site by the second surgical operation. This again leads to tissue damage and recovery time (6). However, these disadvantages can be overcome by the use of biodegradable materials. The most common biodegradable materials are synthetic polyesters which are polylactic acid, polyglycolic acid, polycaprolactone or copolymers thereof (7–10). These aliphatic polyester polymers are biocompatible materials and are degraded by hydrolytic or enzymatic pathways, and this makes them suitable for medical use. Furthermore, the biodegradation rate and mechanical properties can be varied depending on the polymer composition and concentration of the components (11,12).

Polylactic acid (or polylactide, PLA) and polyglycolide (or poly(glycolic acid), PGA) have glass transition temperatures (Tg) above room temperature and this makes them hard and brittle. However, polycaprolactone (PCL) is a crystal and has a low glass transition temperature, so is tough but has a modulus an order of magnitude smaller than PLA (13). However, these independent features cannot provide ideal conditions for all applications. In order to eliminate the disadvantages of properties of the material, the properties of the obtained materials must be adjustable. The mechanical properties of the polymers are characterized as a competition between elastic and plastic deformation and the preparation of different polymer mixtures is among the alternative methods for adjusting the material properties obtained. The new polymer mixture obtained by combining polymer structures with different properties provides the possibility of obtaining new polymers with different properties depending on the mechanical properties of the components and the microstructure of the mixture and the interface between the phases. In addition to the interface and mixture microstructure between these polymer mixtures and the phases, different properties can be obtained which depend precisely on the mechanical properties of the components (14–17).

Most natural materials are composites of inorganic and organic components arranged in complex structures. The bone is composed of collagen matrix (organic) strengthened with hydroxyapatite (HAp) (inorganic). Bone cells, in other words, osteoblasts, osteocytes, osteoclasts, and osteoprogenitor cells are present in and around the matrix. While bioactive materials bind physically and chemically to the bone, a bioabsorbable material is slowly absorbed, ideally substituted by new bone formation. In addition, osteoconductive materials (such as calcium orthophosphate) are suitable for adherence, growth, proliferation and spread of bone cells, while osteoinductive materials (such as hydroxyapatite) are effective in the growth and maturation of primitive stem cells or immature bone cells. Also, the inorganic part in the organic matrix not only improves the mechanical properties of the obtained materials but also supports the physical environment (18–20).

Many methods have been developed to synthesize HAp particles. Some of these are precipitation method (21–23), sol-gel method (24,25), hydrothermal technique (26), emulsion technique (27), biomimetic precipitation (28,29) and electrophoretic precipitation (30). Among these methods, the sol-gel allows controlling the purity, composition, and size of the particles to be produced at the molecular level. The crystallization of the amorphous particles produced in this method may require a high temperature. The thermal treatment required for the production of particles having a crystal structure is not required in the hydrothermal method which is operated at high pressure (31).

In recent years, electrospinning method is one of the production methods that are frequently used in the production of tissue scaffolds (32). The length, width, orientation and total porosity of the nanofibers having submicron fineness can be adjusted to the extent expected by this method. Thus, it is provided to form three-dimensional structures very similar to the extracellular matrix form by arranging these fibers dispersedly side by side and on top of each other. Situations such as the fact that as the surface properties become more functional as the diameter of polymer fibers become smaller, increasing in mechanical performance, providing high porousness and high surface area, which are important in terms of tissue engineering emerge (33). In addition, the fact

that it requires a small amount of raw material in the studies carried out by the electrospinning method provides superiority in terms of production. It is also possible to accelerate tissue formation by biological factors that can be added during or after the electrospinning process (34,35).

Most of the biocompatible and biodegradable polymers can be obtained by electrospinning (36). However, many devices can often cause bacterial infections (37). Also, infection of the treatment site should be prevented so that the trauma in the areas of usage of the biomaterials can be eliminated as soon as possible and the wound closes quickly. For this purpose, antibiotic treatment is applied before and after the operation. However, there are also cases where infection develops. The presence of infections can be a serious challenge in the tissue engineering process. The materials obtained in order to minimize these and similar conditions can be gained anti-bacterial (AB) properties. In particular, the use of drug release composites for implant coating is effective in the prevention and treatment of these infections and diseases (38,39).

Antibacterial agents can be classified as inorganic and organic, and the anti-bacterial materials described in the literature include direct impregnation with antibiotics and the use of silver or antibiotic-coated polymer layers. Silver-based anti-microbials have attracted attention due to their non-toxicity for mammalian cells and the anti-microbial effect of silver ions. The addition of Ag^+ ions into polymeric materials has been used extensively for several years. Ag^+ layer decreased infections especially in urinary and venous catheters (40–42). In addition, the antibacterial property can be obtained from natural materials. Chitosan is obtained by deacetylation of chitin which is obtained from shrimp shells (43). Chitosan is widely used in wound treatment. Also, it can be sorted as medical artificial skin, surgical sutures, anti-fungal, anti-bacterial effects, etc. and in-vivo tests have shown that chitosan does not have any adverse effects to the human body (44).

In this study, bioactive Hap particle prepared by wet precipitation method was added to the biodegradable organic PLA / PCL blend to form a composite structure and fiber was obtained by electrospinning method by adding different ratios of various antibacterial agents. The chemical structure of HAp particle obtained by precipitation method was investigated by Fourier Transform Infrared Spectroscopy (FT-IR), its crystal structure was examined by X-ray

Diffraction and its morphology was analyzed by Scanning Electron Microscopy (SEM). The molecular structure of the obtained polymer was analyzed by FT-IR analysis. Morphology of biocomposite nanofibers was examined by SEM. Antibacterial efficiencies were investigated against *Staphylococcus aureus* (Gram-positive) and *Escherichia coli* (Gram-negative) by ASTM: E2149–01. In addition, the obtained biocomposites were characterized thermal behavior, mechanical properties, and in vitro degradation test. In particular this study involves setting up anti-bacterial agent parameters in order to achieve an anti-bacterial biocomposite nano-fiber materials to be used various area. Electrospinning process has been investigated by authors in the literature demonstrate that electrospinning process is very important for polymer and their properties. In consequence, according to the author it is important to add their contribution to the literature on the topic, and a novel anti-bacterial biocomposite nano-fiber is suitable for further studies as an alternative material for tissue engineering.

EXPERIMENTAL SECTION

Materials
The poly(lactic acid) (PLA, 6252D, M_w = 150.000 (45)) was obtained from Nature-works Co., Ltd. (USA) and the Polycaprolactone (PCL, average M_w 80.000) was obtained from Aldrich. Both polymers were used as received. Chloroform (analytical grade) was supplied by Merck and used without further purification. Diammonium hydrogen phosphate (($NH_4)_2HPO_4$, Merck), calcium nitrate tetrahydrate ($Ca(NO_3)_2.4H_2O$, Merck), ammonium hydroxide (NH_4OH, Merck) were used for the HAp powder synthesis. All reagents were of analytical reagent grade and used without further purification. Deionized water was used in all synthetic steps. Chitosan (Sigma-Aldrich), silver-based inorganic antimicrobial agent (2.5 wt% Ag^+, AJ10N, Sinanen Zeomic Co. Ltd.) were used as anti-bacterial agents.

Preparation of HAp powder and biocomposite solution, electrospinning process
Hydroxyapatite nanoparticles were synthesized by the wet chemical method (46). 200 mL 3 M diammonium hydrogen phosphate was stirred in a beaker at room temperature and 200 mL 5 M calcium nitrate tetrahydrate was added drop wise over 2 h. The pH of the system was maintained at 10.8 throughout the stirring process, by using 25% NH_4OH solution. The mixture was allowed to remain stirred overnight. A white precipitate was formed. A

milky and somewhat gelatinous precipitate was held at 100 °C for 12 h in the oven followed by calcination at 750 °C for 8 h. The prepared powder was used for further characterization. The schematic presentation of the procedure is given in Figure 1. This precipitation reaction for the synthesis of hydroxyapatite nanoparticles was first proposed by Yagai and Aoki, as indicated by Bouyer et al. (2000).
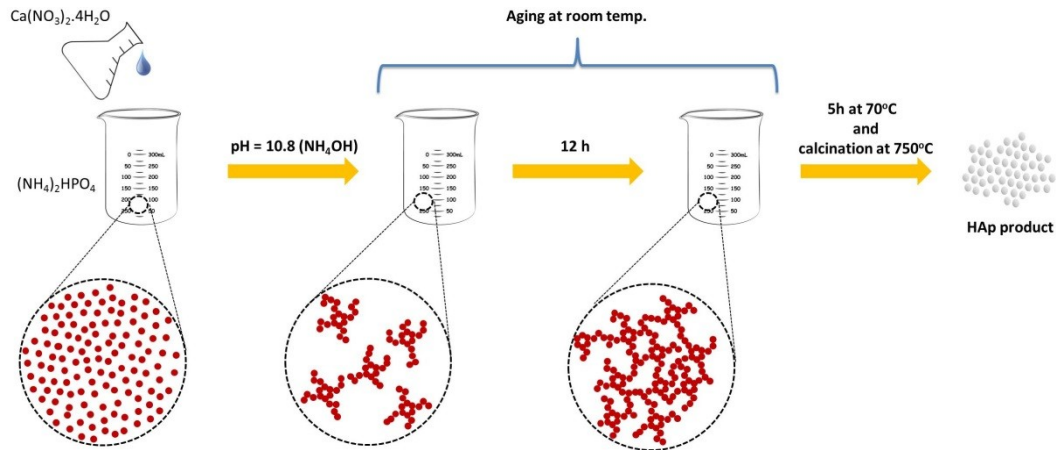

Figure 1: Flowchart of hydroxyapatite powder preparation by wet chemical method.

The required amounts of PLA and PCL were dissolved in chloroform. The PLA solution was then transferred into the PCL solution drop wise with continuous stirring. After all the PLA solution was transferred into the PCL solution, the resultant mixture was then stirred for 1 h. PLA and PCL blends were prepared with a total polymer mass fraction of 10%. The required prepared HAP was then added into the dissolved PLA/PCL blend in the small portion. The mixture was then ultrasonically stirred for 15 min to make sure that the HAp particles fully dispersed in the organic solution. In the next step, chitosan and/or Ag^+ (as AJ10N) were added and stirred for 1 hour. Each final nanofiber solutions were designed as shown in Table 1. Then, the nanocomposite nanofibers were produced by an electrospinning method.

Electrospinning was performed using an Inovenso, NE300 model Electrospinning Machine. A high voltage supply was used to generate an electric field, in the range 20–25 kV between needle and collector. The biocomposite solution was placed in a 10 mL syringe and a pump system was used to feed the solution through the needle at 5 mL/h flow rates. The needle was set up vertically in the spinneret. The collector was a rectangular copper plate covered with aluminum foil and located 15 cm from the needle tip and electrospinning time of 30 min were used. The electrospinning process was performed at room temperature (25 °C) and controlled humidity value (~50% R.H.).

Table 1. Composition of organic-inorganic biocomposite materials.

Sample	w/w content in the biocomposite nanofiber mixture					
	Organic matrix			Inorganic matrix	AB Agent, % in solid	
	PLA	PCL	Chloroform	HAp	Chitosan	Ag$^+$
PLA-PCL				–	–	–
CF-0					–	–
CF-1C					1.00	–
CF-2.5C					2.50	–
CF-5C					5.00	–
CF-0.25A					–	0.25
CF-0.5A	4	6	90	1	–	0.50
CF-1A					–	1.00
CF-2.5A					–	2.50
CF-5A					–	5.00
CF-1C-0.25A					1.00	0.25
CF-2.5C-0.25A					2.50	0.25
CF-1.5C-0.25A					1.00	0.50

Characterization

Structural characterization and functional groups identification of the obtained HAp particle was done using Fourier Transform Infrared Spectroscopy (FT-IR) analyses with a Tensor 27 model spectrophotometer. X-ray Diffraction (XRD) patterns were collected using Bruker Axs d8 advance model XRD. The morphological pattern of granules was observed using a Scanning Electron Microscope (ZEISS-LEO 1430 SEM equipment).

The FTIR spectra of the organic matrix were recorded on Tensor 27 model spectrophotometer at ambient temperature. The sample was scanned at 16 scans at wavenumber range of 400-4000 cm^{-1}. The morphological aspect of the biocomposite nanofibers was measured by a scanning electron microscope (ZEISS-LEO 1430 SEM equipment). Thermogravimetric analysis (TGA) of the obtained samples was performed by using a Seiko SII TG/DTA 7200 thermogravimetric analyzer. The tests were run from 30 to 800 $^{\circ}$C with a heating rate of 10 $^{\circ}$C/min under a nitrogen atmosphere. Tensile test was carried out on Shimadzu Autograph AGS-X series at ambient environment. The specimens were cut into approximate dimensions of 65 mm × 10 mm. The cross head speed was 10 mm/min and load applied was 10 N/mm^2. In vitro degradation studies were carried out in a simulated bodily fluid (SBF) at 37 $^{\circ}$C. SBF solution was prepared with the reagents NaCl, NaHCO$_3$, KCl, K$_2$HPO$_4$·3H$_2$O, MgCl$_2$·6H$_2$O, CaCl$_2$·2H$_2$O and Na$_2$SO$_4$ into distilled water (47). Samples were immersed in SBF solution for time periods of 144, 288, 432, 576 and 720

hours. Before the weight losses were determined, the samples were extracted from the SBF solution, and left to dry at room temperature to a stable mass. Three samples were measured for the obtained weight loss value. The modified American standard ASTM: E2149–01 was used to investigate the antibacterial activity by using facultative gram-negative *Escherichia coli* (*E. Coli,* ATCC 11775) and gram-positive *Staphylococcus aureus (S. aureus,* ATCC 25923).

RESULTS AND DISCUSSION

Hydroxyapatite powder

The wavenumber of the peaks observed in the FT-IR spectrum of the wet chemically precipitated HAp powder in Table 2 are reported as details about which types of vibration they are and to which organic groups they belong.

The FT-IR spectrum showed a characteristic peak of hydroxyapatite in Figure 2; the stretching and bending vibrations of water (corresponded to adsorbed water) were observed at 3448 cm^{-1} and 1644 cm^{-1} wavenumbers, respectively. The peaks appeared at 3572 cm^{-1} and 636 cm^{-1} wavenumbers, respectively, was corresponded to the stretching and bending vibrations of the (OH−) ions in the molecular structure of HAp. Characteristic bands that belong to the (PO$_4^{3-}$) ions were detected at 1096 cm^{-1}, 1036 cm^{-1}, 962 cm^{-1}, 604 cm^{-1}, 596 cm^{-1} wavenumber values (22,48). These results confirm the synthesis of HAp structure.

The peaks in the XRD spectra (Figure 3)

demonstrated that hexagonal hydroxyapatite (HAp, syn., $Ca_5(PO_4)3OH$) phase with COD 9011092 card number exist in the sample. The obtained results with narrow and sharp peaks are the signs of well-developed crystals.

Table 2. FTIR wavenumbers and observed assignments of HAp powder.

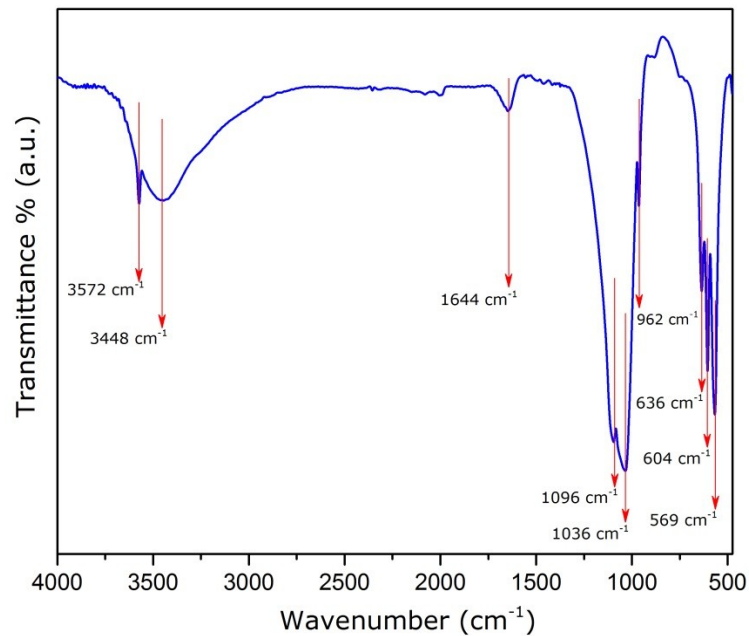| Assignments	Observed peak (cm^{-1})	Definition
v_s –OH	3572	OH^- structural
v_{as} H2O	3448	Stretching vibrations of H_2O
δ H2O	1644	bending vibrations of H_2O
v_{as} P-O	1096	PO_4 bending
v_{as} P-O	1036	PO_4 bending
v_s P-O	962	PO_4 tension
v_s –OH	636	OH structural
δ O-P-O	604, 596	PO_4 of bending

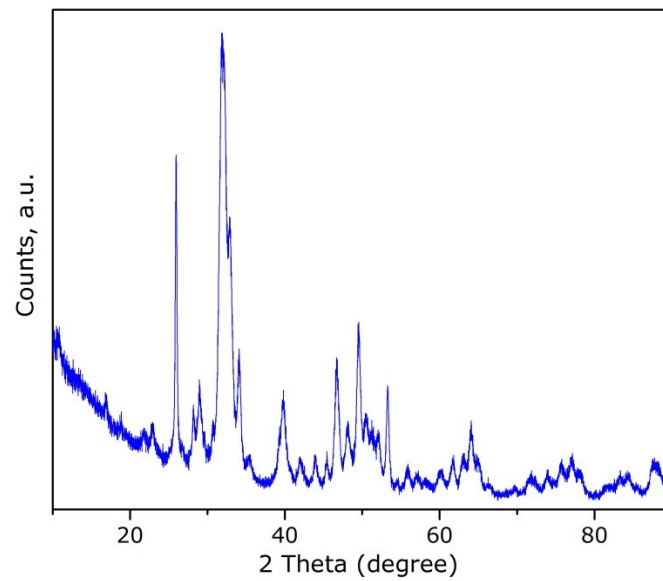**Figure 2:** FT-IR spectrum of the hydroxyapatite powder sample.

Figure 3: XRD results of the hydroxyapatite powder sample.

Scanning Electron Micrograph (SEM) of the obtained HAp is shown in Figure 4. As can be seen from the morphologies of particles, there is a distribution of small particles and large agglomerates. The particle size ranged between 1 and 15 μm (120 particles were measured). These agglomerates consist of fine particles.
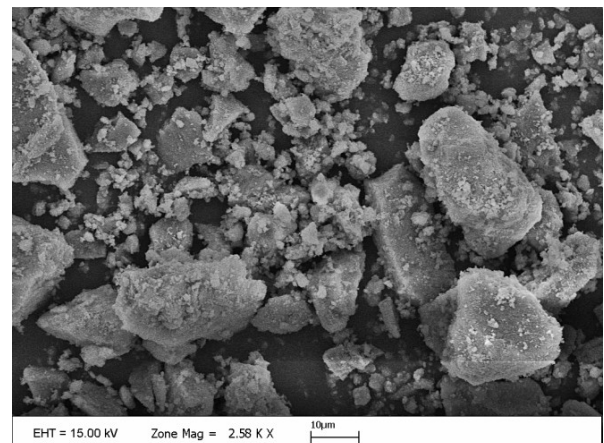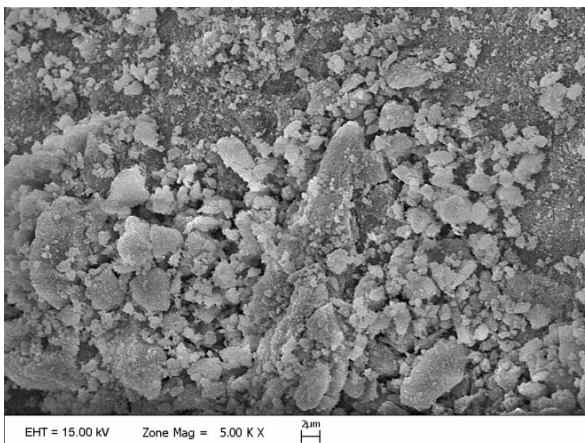

Figure 4: SEM images of the hydroxyapatite powder sample.

Organic matrix and biocomposite materials

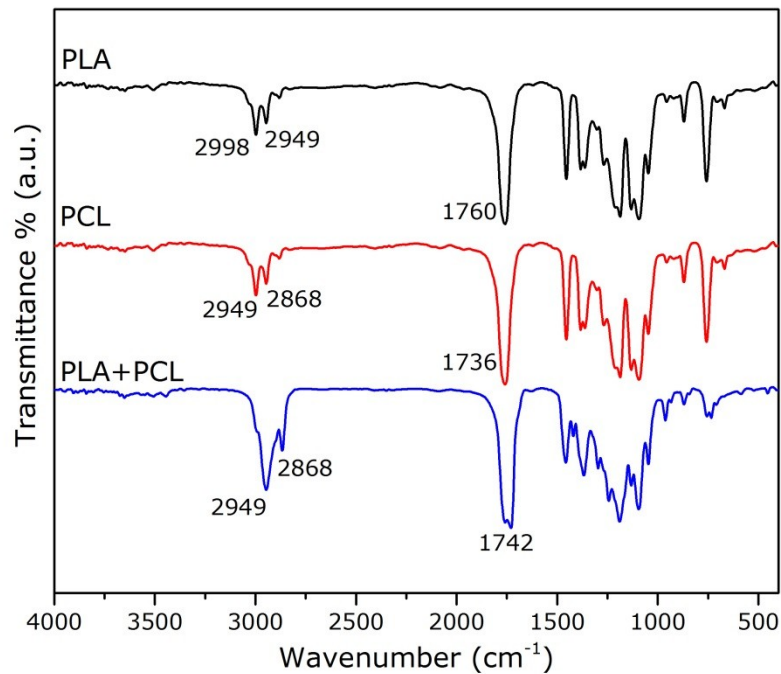FT-IR analysis gives information on the molecular structure of the PLA, PCL and PLA/PCL blends.

Figure 5: FTIR spectra of PLA, PCL, PLA/PCL blend.

The FT-IR spectrum of the polymer (Figure 5) shows peaks in the 3000–2900 cm^{-1} and 1760 cm^{-1} of PLA and 2949, 2869 and 1736 cm^{-1} of PCL range due to CH (CH$_2$ and CH$_3$) stretching and due to ester −C=O group stretching, respectively. In the PLA/PCL blend, these peaks were found in the neutralized regions of 2949, 2868 and 1742 cm^{-1}.

Figure 6 shows SEM images of electrospun ultrafine biocomposite nanofibers. The diameter of the obtained electrospun nanofibers was around 172 ± 90 nm. It was observed that HAp was homogeneously formed on the nanofiber material. The SEM results suggest that HAp particles can be homogeneously incorporated with PLA+PCL matrix.
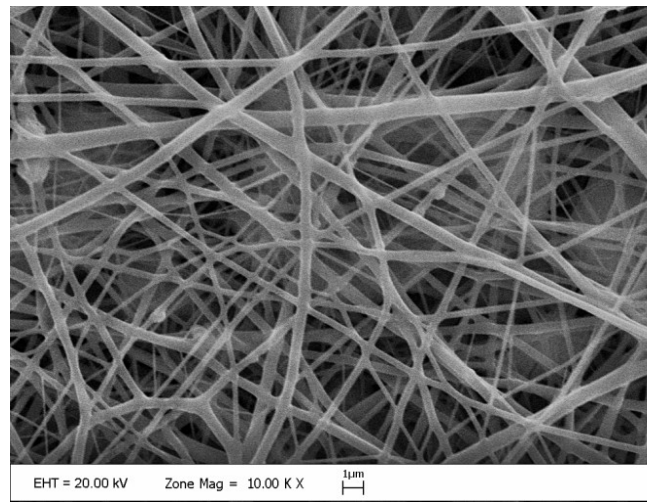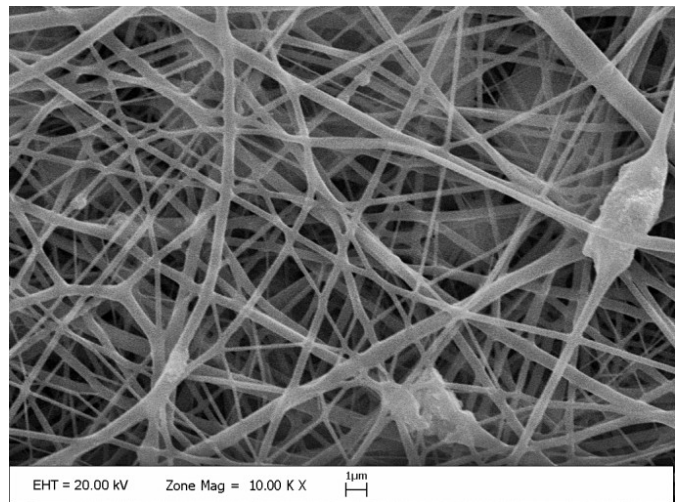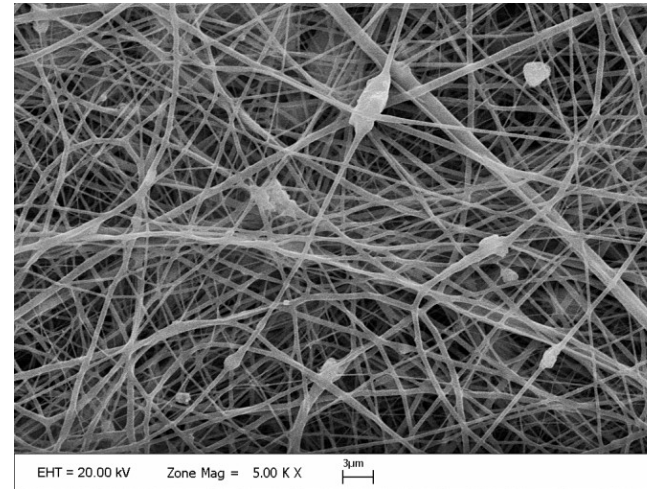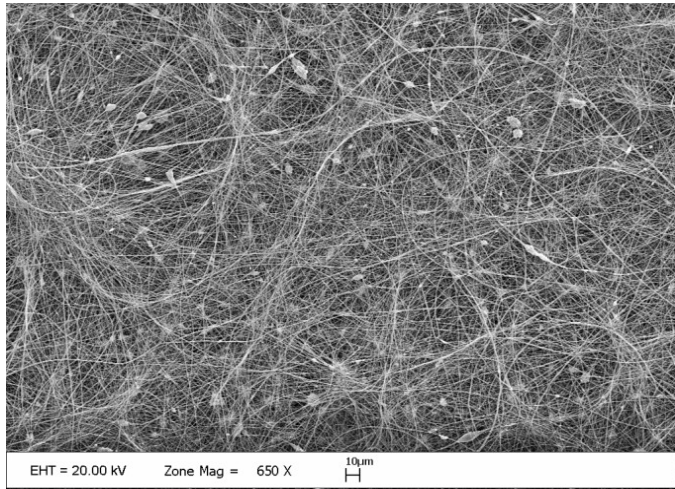
Figure 6. SEM images of the biocomposite nanofibers containing Hap.

The thermal properties of the samples were evaluated with the TGA analysis. When we examine the TGA and differential thermogravimetric (DTG) thermograms for the sample PLA/PCL, CF-0 and CF-1C-0.25A given in Figure 7, the main weight loss for PLA/PCL organic matrix was observed in the temperature range 265 $^{\circ}$C – 456 $^{\circ}$C due to the decomposition of polymer structure. The residual mass might due to PCL, which may not completely decompose over 700 $^{\circ}$C. The DTG curve of PLA/PCL organic matrix follows a two-stage at 367°C and 411°C respectively, consistent with the result shown in the literature (49,50). The degradation temperature of the composite sample for the sample CF-0 increase with the adding of HAP to the PLA/PCL organic matrix, the decomposition of the sample CF-0 starts at around 279 °C and completes at 462 °C the DTG curve of the sample CF-0 shows a two-stage thermal decomposition at 372 °C and 415 °C. The degradation temperature of the AB composite sample for the sample CF-1C-0.25A increase with the adding of HAP and AB agents to the PLA/PCL organic matrix, the decomposition of the sample starts at around 301 °C and completes at 463 °C the DTG curve of the sample shows a two-stage peak at 376 °C and 416 °C. The temperature of the main degradation is shifted towards a higher value when HAP and HAP/AB agents are used compare to the PLA/PCL organic matrix (51).
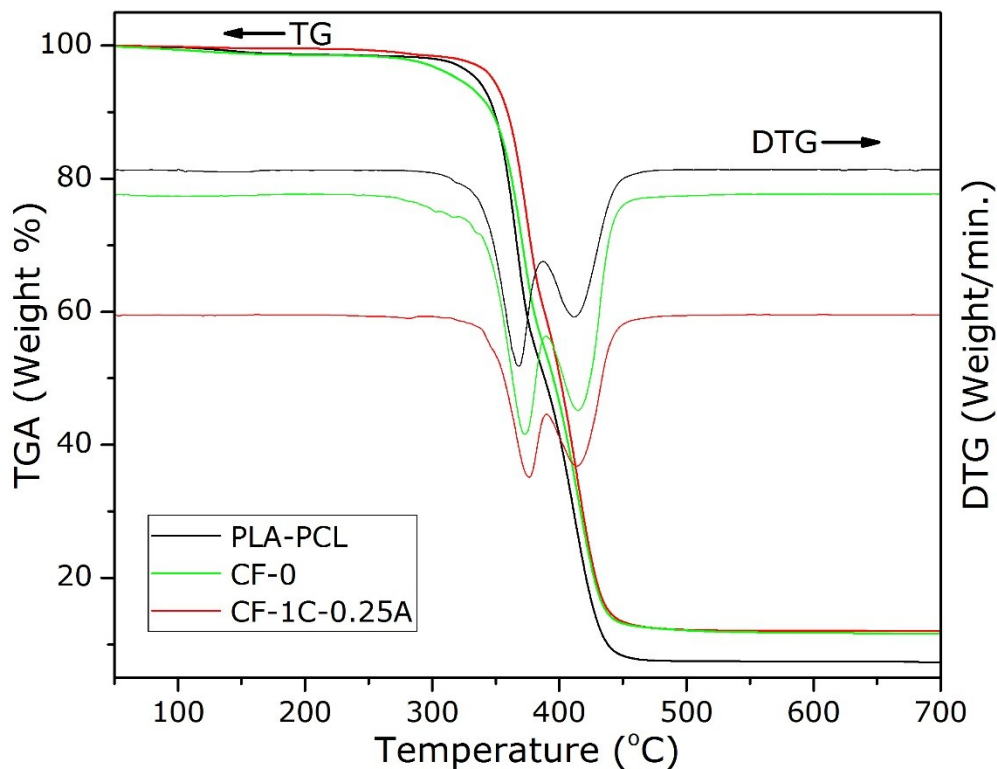
Figure 7: Thermo-gravimetric analysis (TGA) thermograms for the samples.

According to the literature Hap particle which is thermally stable up to 1300 $^{\circ}$C (52). Therefore, the residual mass remaining in these samples were assigned to the Hap particle and AB agents. 10 wt.% HAP particle and 10 wt.% HAP particle, 1 wt.% chitosan, and 0.25 wt.% Ag were added to PLA/PCL organic matrix during the preparation of sample CF-0 and CF-1C-0.25A, respectively. According to the obtained results of the TGA measurement, it was detected that the percentage of residual in sample CF-0 and CF-1C-0.25A were 11.25 and 12.06 wt. %, respectively (Table 3), which is in accordance with their initial addition. In this case, the content of HAp particle and AB agents in the final composite samples can be precisely

manipulated with predetermined HAp particle and AB agents concentrations in the mixed solution to fabricate fibers through electrospinning.

Table 3. Thermal analysis results for the samples.

Sample	Weight Loss Temperature (^{O}C)			Residual (%)
	$T_{10\%}$	$T_{30\%}$	$T_{50\%}$	
PLA-PCL	342	366	387	5.25
CF-0	347	371	395	11.75
CF-1C-0.25A	359	378	401	12.06

In Table 3 the results obtained from the TGA curves of Figure 7 are summarized. The temperature corresponding to the degradation of 10 – 30 and 50 wt. % of the samples ($T_{10\%}$, $T_{30\%}$, $T_{50\%}$) is higher than for the sample PLA-PCL, indicating that the HAP particle and AB agents addition improve the thermal stability of PLA-PCL organic matrix.

In order to determine the mechanical properties of the obtained samples, tensile strength and elongation at break tests were performed. Tensile strength value of the sample PLA-PCL and CF-0 were 21.20 and 24.54 MPa respectively. As it can be observed in Figure 8, the addition of HAP particle leads to a clear change in the fracture behavior of PLA-PCL. In addition, there was not a noticeable difference in tensile strength and elongation at break between the sample CF-0 and CF-1C-0.25A containing AB agents.
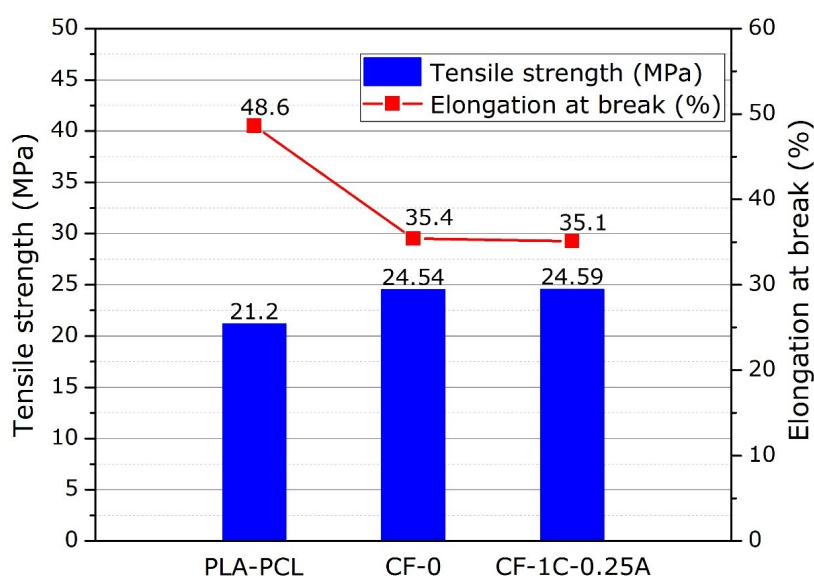

Figure 8: Results of the tensile strength and elongation-at-break of the samples.

It is known from the literature that PCL degradation time can be 12 or 24 months, according to its molecular weight, while PLA degradation time can be from 15 days up to 6 months, according to its molecular weight (53). The changes in weight loss of the samples as a function of degradation time in SBF are shown in Figure 9. After 144-hour of immersion in SBF, the mass loss was less than 2% for the sample PLA-PCL, less than 3% for the samples CF-0 and CF-1C-0.25A. After 720-hour of immersion in SBF, a linear mass loss was observed for all the samples. The highest weight loss was determined for CF-0 and CF-1C-0.25A whereas the lowest for the sample PLA-PCL. According to the obtained results, degradation rate of the biocomposite samples increased with HAP particle and AB agents added to PLA-PCL organic matrix.
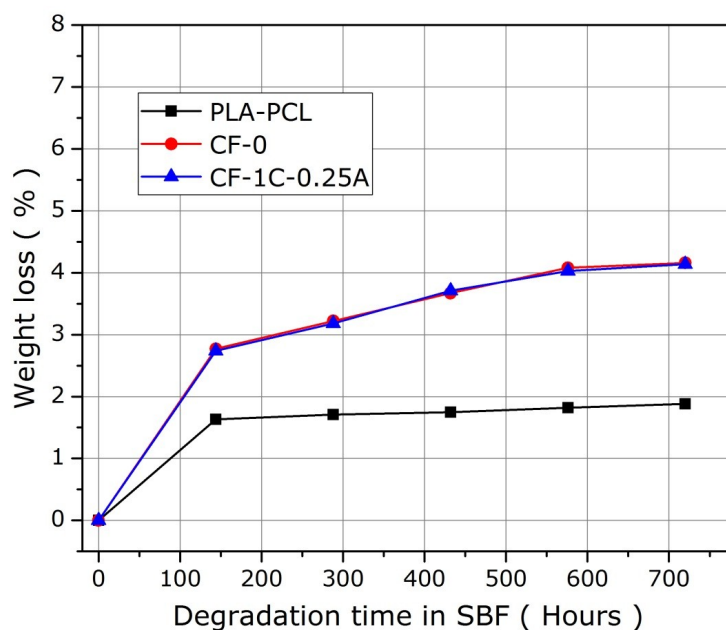
Figure 9: Weight loss of the samples as a function of degradation time in SBF solution.

According to the modified E2149-10 standard, anti-microbial tests were performed at 12 and 24 hour contact times. An obtained average reduction of colony formation unit (CFU) and Log reduction for *E.coli* and *S.aureus* bacteria samples were shown in Tables 4 and 5, and change of % reduction in bacteria population compared to anti-bacterial agent were shown in Figure 10 and visual results were presented in Figure 11. Anti-bacterial efficiency was investigated by adding different amounts of chitosan and/or Ag⁺ to the biocomposite structure prepared as anti-bacterial agent. Increased rates of both AB agents increased the antibacterial effect.

The sample containing 5% chitosan provided a reduction in the bacterial population of up to 60% at the end of 24 hours against both bacterial species, while similar results could be achieved in the sample containing 0.25% Ag⁺ under the same conditions. In the biocomposite

sample containing 1% Ag⁺, an effective AB property is achieved and a decrease in the 99.99% bacterial population is observed.

The biocomposite nanofibers containing chitosan inhibit the growth of bacterial populations considering AB efficiency and show that chitosan has a bacteriostatic effect compared to Ag⁺.

It was found that samples containing 1% chitosan and 0.25% Ag⁺ separately reduced bacterial populations at the end of 12 hours by 2.5% and 40%, respectively. However, it was determined that composite nanofibers prepared by using these amounts of AB agents together, decreased at the end of the same period in approximately 80% bacterial population. It was concluded that both AB agents were in compliance with each other and had effects on test bacteria with a synergistic interaction.

Table 4: *Anti-Bacterial activity against E. coli of biocomposite nanofibers.*

Sample	Initially (CFU/mL)	Escherichia coli					
		After 12h			After 24h		
		(CFU/mL)	Average Reduction, Log_{10}	Average CFU Reduction, %	(CFU/mL)	Average Reduction, Log_{10}	Average CFU Reduction, %
Control, Blank		8.85×10^7	–	–	2.17×10^8	–	–
CF-0		8.52×10^7	–	–	2.11×10^8	–	–
CF-1C		1.19×10^6	0.01	2.46	8.50×10^5	0.16	30.32
CF-2.5C		1.09×10^6	0.05	10.83	6.10×10^5	0.30	50.00
CF-5C		0.77×10^6	0.20	36.89	4.68×10^5	0.42	61.64
CF-0.25A		0.72×10^6	0.23	40.98	4.24×10^5	0.46	65. 25
CF-0.5A	1.22×10^6	0.49×10^6	0.40	59.84	3.48×10^5	0.54	71.48
CF-1A		0.59×10^5	1.32	95.16	< 20	4.78	>99.99
CF-2.5A		< 20	4.78	>99.99	< 20	4.78	>99.99
CF-5A		< 20	4.78	>99.99	< 20	4.78	>99.99
CF-1C-0.25A		2.93×10^5	0.62	75.98	< 20	4.78	>99.99
CF-2.5C-0.25A		2.43×10^5	0.70	80.08	< 20	4.78	>99.99
CF-1C-0.5A		9.65×10^4	1.10	92.09	< 20	4.78	>99.99

Table 5: Anti-bacterial activity against *S. aureus* of biocomposite nanofibers.

| Sample	Initially (CFU/mL)	Staphylococcus Aureus					
		After 12h			After 24h		
		(CFU/mL)	Average Reduction, Log_{10}	Average CFU Reduction, %	(CFU/mL)	Average Reduction, Log_{10}	Average CFU Reduction, %
Control, Blank		$7,25 \times 10^7$	–	–	1.98×10^8	–	–
CF-0		$6,92 \times 10^7$	–	–	$2,03 \times 10^8$	–	–
CF-1C		1.35×10^6	< 0.01	2.17	1.02×10^6	0.13	26.09
CF-2.5C		1.26×10^6	0.04	8.70	0.70×10^6	0.29	49.28
CF-5C		0.90×10^6	0.19	34.78	0.54×10^6	0.41	60.87
CF-0.25A		0.83×10^6	0.22	39.86	0.52×10^6	0.42	62,32
CF-0.5A	1.38×10^6	0.61×10^6	0.35	55.80	0.37×10^6	0.57	73.19
CF-1A		0.15×10^6	0.96	89.13	< 20	4.84	>99.99
CF-2.5A		< 20	4.84	>99.99	< 20	4.84	>99.99
CF-5A		< 20	4.84	>99.99	< 20	4.84	>99.99
CF-1C-0.25A		0.40×10^6	0.54	71.01	< 20	4.84	>99.99
CF-2.5C-0.25A		0.27×10^6	0.71	80.43	< 20	4.84	>99.99
CF-1C-0.5A		0.12×10^6	1.06	91.30	< 20	4.84	>99.99
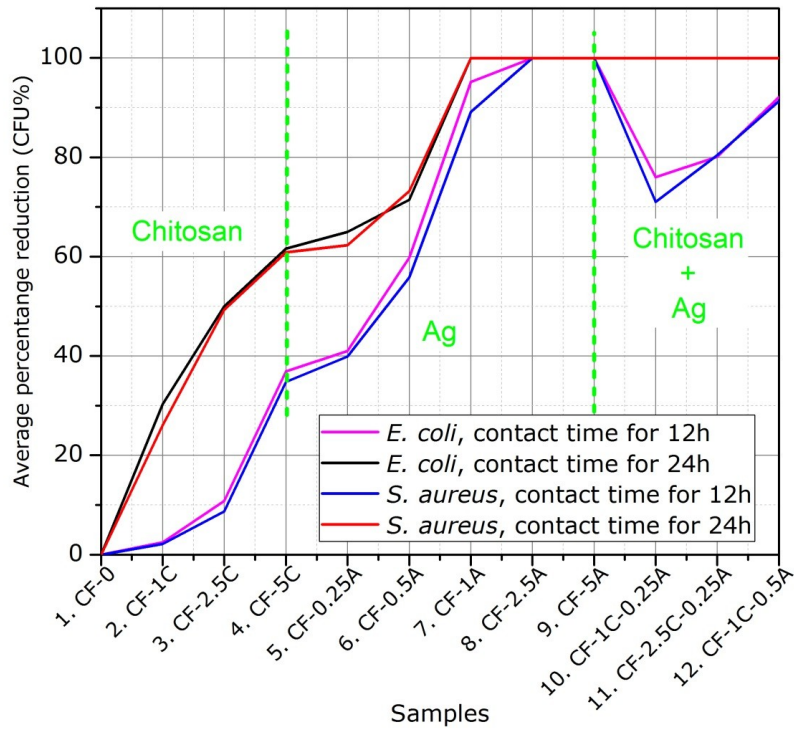
Figure 10: According to the contact time, the percentage of CFU reduction graph for biocomposite nanofibers against *E. coli* and *S. aureus*.

Figure 11 shows the respective 90 mm plates of the CF-0 and CF-1C-0.25A samples antimicrobial activity after 24 h of incubation for *S. aureus* and *E. coli* (from the diluted test solution). Each white round dot in the photographs shows a CFU. Biocomposite samples containing anti-bacterial agent suppressed the growth of the bacterial population compared to the control group and eliminated live bacteria.
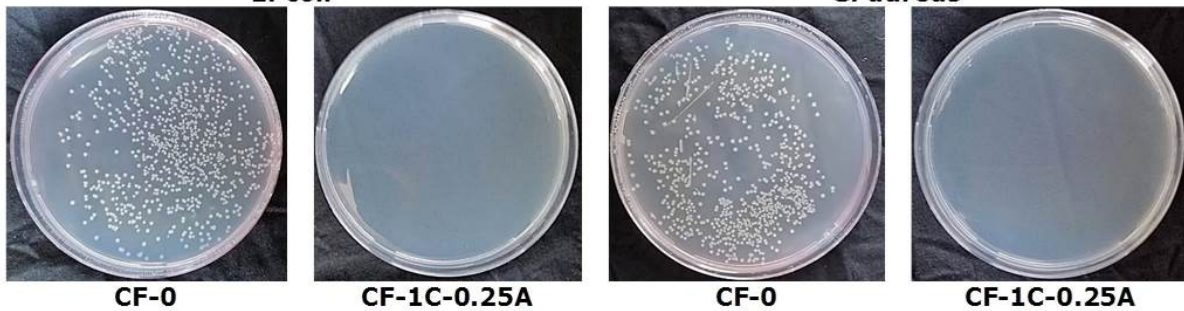

Figure 11: Antibacterial activity for E. coli and S. aureus (from the diluted test solution) in the Petri dishes.

CONCLUSION

In this study, HAp particles synthesized by wet precipitation method were added to biodegradable PLA/PCL matrix and biocomposite nano-fibers were prepared by providing anti-bacterial properties with chitosan and/or Ag$^+$. The efficiencies of *E. coli* and *S. aureus* bacteria at different contact times depending on the type and amount of AB agent were investigated in detail and efficient AB agent amounts were determined. AB efficiency has been carried out from antic times to the present and it has been found that there is a synergistic effect in the use of Ag$^+$, chitosan, in which a broad spectrum of AB features and bacterial species do not gain immunity. Thus, the decrease in the 99.99% bacterial population, which can be obtained with min 1% Ag$^+$, was provided by using 1% chitosan and 0.25% Ag$^+$, and similar results were obtained for both bacterial species. In several studies, it is suggested that the amounts of Ag$^+$ used should be reassessed to minimize in a controlled manner. There is sufficient evidence that long-term adverse effects may occur from exposure to silver in an uncontrolled and unconscious manner (54). When taking this situation into account, the most striking result of this study is the quantitative determination of antibacterial efficiency by combining chitosan which is a natural polymer, biodegradable, safe and non-toxic biocompatible chitosan with Ag$^+$. It was determined that thermally stable properties increased with HAp particle in the biocomposite fibers. Furthermore in vitro degradation studies have demonstrated, degradation rate of the biocomposite samples increased with HAP particle, but AB agents in the biocomposite were not affected these results. According to the mechanical test HAp particle and AB agents were added to the sample PLA-PCL, it was resulted that the biocomposite samples become more rigid and the elongation at break is slightly reduced.

Finally, the experimental results clearly show that the obtained biocomposite nano-fibers allow for the development of new composite materials with anti-bacterial properties, good mechanical strength, thermally stable. The results also confirm the great potential of biodegradable, biocompatible and bioactive fibers for antibacterial application.

COMPLIANCE WITH ETHICAL STANDARDS

Conflict of interest
The author declares that they have no conflict of interest.

REFERENCES

1. Leó B, Jansen JA. Thin calcium phosphate coatings for medical implants. Thin Calcium Phosphate Coatings for Medical Implants. 2009.

2. Bottino MC, Thomas V, Schmidt G, Vohra YK, Chu TMG, Kowolik MJ, et al. Recent advances in the development of GTR/GBR membranes for periodontal regeneration - A materials perspective. Dent Mater [Internet]. 2012;28(7):703–21. Available from: http://dx.doi.org/10.1016/j.dental.2012.04.022

3. Dahlin C, Linde A, Gottlow J, Nyman S. Healing of bone defects by guided tissue regeneration. Plast Reconstr Surg. 1988;

4. Hitti RA. Guided Bone Regeneration in the Oral Cavity: A Review. Open Pathol J. 2011;5(1):33–45.

5. Retzepi M, Donos N. Guided Bone Regeneration: Biological principle and therapeutic applications. Clin Oral Implants Res. 2010;21(6):567–76.

6. Hämmerle, C.H. & Jung RE. Bone augmentation by means of barrier membranes. Periodontology. 2000;33:36–53.

7. Sculean A, Nikolidakis D, Schwarz F. Regeneration of periodontal tissues: Combinations of barrier membranes and grafting materials - Biological foundation and preclinical evidence: A systematic review. J Clin Periodontol. 2008;35(SUPPL. 8):106–16.

8. Gentile P, Chiono V, Tonda-Turo C, Ferreira AM, Ciardelli G. Polymeric membranes for guided bone regeneration. Biotechnol J. 2011;6(10):1187–97.

9. Geurs NC, Korostoff JM, Vassilopoulos PJ, Kang T-H, Jeffcoat M, Kellar R, et al. Clinical and Histologic Assessment of Lateral Alveolar Ridge Augmentation Using a Synthetic Long-Term Bioabsorbable Membrane and an Allograft. J Periodontol. 2008;79(7):1133–40.

10. Milella E, Barra G, Ramires PA, Leo G, Aversa P, Romito A. Poly(L-lactide)acid/alginate composite membranes for guided tissue regeneration. J Biomed Mater Res. 2001;57(2):248–57.

11. Hirenkumar M, Steven S. Poly Lactic-co-Glycolic Acid (PLGA) as Biodegradable Controlled Drug Delivery Carrier. Polymers (Basel). 2012;3(3):1–19.

12. Vert M. Aliphatic polyesters: Great degradable polymers that cannot do everything. Biomacromolecules. 2005;6(2):538–46.

13.   Nofar M, Sacligil D, Carreau PJ, Kamal MR, Heuzey MC. Poly (lactic acid) blends: Processing, properties and applications. Int J Biol Macromol [Internet]. 2019;125:307–60. Available from: https://doi.org/10.1016/j.ijbiomac.2018.12.002

14.   Patrício T, Domingos M, Gloria A, D'Amora U, Coelho JF, Bártolo PJ. Fabrication and characterisation of PCL and PCL/PLA scaffolds for tissue engineering. Rapid Prototyp J. 2014;20(2):145–56.

15.   Latthe SS, Imai H, Ganesan V, Rao AV. Superhydrophobic silica films by sol-gel co-precursor method. Appl Surf Sci. 2009;256(1):217–22.

16.   Patrício T, Bártolo P. Thermal stability of PCL/PLA blends produced by physical blending process. Procedia Eng [Internet]. 2013;59:292–7. Available from: http://dx.doi.org/10.1016/j.proeng.2013.05.124

17.   Broz ME, VanderHart DL, Washburn NR. Structure and mechanical properties of poly(D,L-lactic acid)/poly(ε-caprolactone) blends. Biomaterials. 2003;24(23):4181–90.

18.   Furukawa T, Matsusue Y, Yasunaga T, Nakagawa Y, Okada Y, Shikinami Y, et al. Histomorphometric study on high-strength hydroxyapatite/poly(L-lactide) composite rods for internal fixation of bone fractures. J Biomed Mater Res. 2000;50(3):410–9.

19.   Rezwan K, Chen QZ, Blaker JJ, Boccaccini AR. Biodegradable and bioactive porous polymer/inorganic composite scaffolds for bone tissue engineering. Biomaterials. 2006;27(18):3413–31.

20.   Soundrapandian C, Sa B, Datta S. Organic–Inorganic Composites for Bone Drug Delivery. AAPS PharmSciTech. 2009;10(4):1158–71.

21.   Santos MH, Oliveira M de, Souza LP de F, Mansur HS, Vasconcelos WL. Synthesis control and characterization of hydroxyapatite prepared by wet precipitation process. Mater Res. 2006;7(4):625–30.

22.   Yelten-Yilmaz A, Yilmaz S. Wet chemical precipitation synthesis of hydroxyapatite (HA) powders. Ceram Int [Internet]. 2018;44(8):9703–10. Available from: https://doi.org/10.1016/j.ceramint.2018.02.201

23.   Monmaturapoj N. Nano-size Hydroxyapatite Powders Preparation by Wet-Chemical Precipitation Route Particle sizes and density were analyzed by. J Met aterials Miner. 2008;18(1):15–20.

24.   Chai CS, Ben-Nissan B. Bioactive nanocrystalline sol-gel hydroxyapatite coatings. J Mater Sci Mater Med. 1999;10(8):465–9.

25.   Liu DM, Troczynski T, Hakimi D. Effect of hydrolysis on the phase evolution of water-based sol-gel hydroxyapatite and its application to bioactive coatings. J Mater Sci Mater Med. 2002;13(7):657–65.

26.   Manafi SA, Joughehdoust S. Synthesis of Hydroxyapatite Nanostructure by Hydrothermal

Condition for Biomedical Application. J Pharm Sci. 2009;5(2):89–94.

27.   Kimura I. Synthesis of Hydroxyapatite by Interfacial Reaction in a Multiple Emulsion. Res Lett Mater Sci. 2007;2007:1–4.

28.   Tas AC. Synthesis of biomimetic Ca-hydroxyapatite powders at 37 degrees C in synthetic body fluids. Biomaterials. 2000;21:1429–38.

29.   Thamaraiselvi T V., Prabakaran K, Rajeswari S. Synthesis of hydroxyapatite that mimic bone minerology. Trends Biomater Artif Organs. 2006;19(2):81–3.

30.   Shirkhanzadeh m. Direct formation of nanophase HAP on cathodically polarized electrodes.pdf. J Mater Sci Mater Med. 1998;9:67–72.

31.   Nayak AK. Hydroxyapatite synthesis methodologies: An overview. Int J ChemTech Res. 2010;2(2):903–7.

32.   Pham QP, Sharma U, Mikos AG. Review---Electrospinning of Polymeric Nanofibers.pdf. 2006;12(5).

33.   Huang ZM, Zhang YZ, Kotaki M, Ramakrishna S. A review on polymer nanofibers by electrospinning and their applications in nanocomposites. Compos Sci Technol. 2003;63(15):2223–53.

34.   Bhardwaj N, Kundu SC. Electrospinning: A fascinating fiber fabrication technique. Biotechnol Adv. 2010;28(3):325–47.

35.   Tanaka K, Shiga T, Katayama T. Fabrication of hydroxyapatite/PLA composite nanofiber by electrospinning. High Perform Optim Des Struct Mater II. 2016;1(Hpsm):371–9.

36.   Gupta B, Revagade N, Anjum N, Atthoff B, Hilborn J. Preparation of poly(lactic acid) fiber by dry-jet-wet-spinning. I. Influence of draw ratio on fiber properties. J Appl Polym Sci. 2006;100(2):1239–46.

37.   Kurtycz P, Karwowska E, Ciach T, Olszyna A, Kunicki A. Biodegradable polylactide (PLA) fiber mats containing Al2O3-Ag nanopowder prepared by electrospinning technique - Antibacterial properties. Fibers Polym. 2013;14(8):1248–53.

38.   Chou J, Ben-Nissan B, Green DW, Valenzuela SM, Kohan L. Targeting and dissolution characteristics of bone forming and antibacterial drugs by harnessing the structure of microspherical shells from coral beach sand. Adv Eng Mater. 2011;13(1–2):93–9.

39.   Karacan I, Macha IJ, Choi G, Cazalbou S, Ben-Nissan B. Antibiotic Containing Poly Lactic Acid/Hydroxyapatite Biocomposite Coatings for Dental Implant Applications. Key Eng Mater. 2017;758(September):120–5.

40.   Björling G, Johansson D, Bergström L, Strekalovsky A, Sanchez J, Frostell C, et al. Evaluation of central venous catheters coated with a

noble metal alloy—A randomized clinical pilot study of coating durability, performance and tolerability. J Biomed Mater Res - Part B Appl Biomater. 2018;106(6):2337–44.

41. Wu K, Yang Y, Zhang Y, Deng J, Lin C. A ntimicrobial activity and cytocompatibility of silver nanoparticles coated catheters via a biomimetic surface functionalization strategy. Int J Nanomedicine. 2015;10:7241–52.

42. Knetsch MLW, Koole LH. New strategies in the development of antimicrobial coatings: The example of increasing usage of silver and silver nanoparticles. Polymers (Basel). 2011;3(1):340–66.

43. Goy RC, Morais STB, Assis OBG. Evaluation of the antimicrobial activity of chitosan and its quaternized derivative on E. Coli and S. aureus growth. Brazilian J Pharmacogn. 2016;26(1):122–7.

44. Montazer M, Afjeh MG. Simultaneous X-linking and antimicrobial finishing of cotton fabric. J Appl Polym Sci. 2007;103(1):178–85.

45. Hablot E, Dharmalingam S, Hayes DG, Wadsworth LC, Blazy C, Narayan R. Effect of Simulated Weathering on Physicochemical Properties and Inherent Biodegradation of PLA/PHA Nonwoven Mulches. J Polym Environ. 2014;22(4):417–29.

46. Chandrasekar A, Sagadevan S, Dakshnamoorthy A. Synthesis and characterization of nano-hydroxyapatite (n-HAP) using the wet chemical technique. Int J Phys Sci. 2013;8(32):1639–45.

47. Kokubo T, Takadama H. How useful is SBF in predicting in vivo bone bioactivity? Biomaterials [Internet]. 2006;27(15):2907–15. Available from: http://www.ncbi.nlm.nih.gov/pubmed/16448693

48. Grigorjeva L, Millers D, Smits K, Jankovica D, Pukina L. Characterization of hydroxyapatite by time-resolved luminescence and FTIR spectroscopy. IOP Conf Ser Mater Sci Eng. 2013;49(1).

49. Qi H, Ye Z, Ren H, Chen N, Zeng Q, Wu X, et al. Bioactivity assessment of PLLA/PCL/HAP electrospun nanofibrous scaffolds for bone tissue engineering. Life Sci [Internet]. 2016;148:139–44. Available from:http://dx.doi.org/10.1016/j.lfs.2016.02.040

50. Marei NH, El-Sherbiny IM, Lotfy A, El-Badawy A, El-Badri N. Mesenchymal stem cells growth and proliferation enhancement using PLA vs PCL based nanofibrous scaffolds. Int J Biol Macromol. 2016;93:9–19.

51. H. Hoidy W, B. Ahmad M, Jaffar Al- EA, Bt Ibrahim NA. Preparation and Characterization of Polylactic Acid/Polycaprolactone Clay Nanocomposites. Vol. 10, Journal of Applied Sciences. 2010. p. 97–106.

52. Locardi B, Pazzaglia UE, Gabbi C, Profilo B. Thermal behaviour of hydroxyapatite intended for medical applications. Biomaterials. 1993;

53. Pisani S, Dorati R, Conti B, Modena T, Bruni G, Genta I. Design of copolymer PLA-PCL electrospun matrix for biomedical applications. React Funct Polym [Internet]. 2018;124(July 2017):77–89. Available from: https://doi.org/10.1016/j.reactfunctpolym.2018.01.011

54. Sim W, Barnard R, Blaskovich MAT, Ziora Z. Antimicrobial Silver in Medicinal and Consumer Applications: A Patent Review of the Past Decade (2007–2017). Antibiotics. 2018;7(4):93.